Aerosol regional deposition of electronic cigarette emissions using an original ex vivo respiratory model

Yoann Montigaud, Baptiste Manzotti, Sophie Chevrel, Lara Leclerc, Gwendoline Sarry, Anthony Clotagatide, Jérémie Pourchez, Nathalie Prévôt

Aerosol regional deposition of electronic cigarette emissions using an original *ex vivo* respiratory model

Yoann Montigaud[1], Baptiste Manzotti[1], Sophie Chevrel[1], Lara Leclerc[1], Gwendoline Sarry[1], Anthony Clotagatide[2,3], Jérémie Pourchez[1], Nathalie Prévôt[2,3]

[1]Mines Saint-Etienne, Univ Lyon, Univ Jean Monnet, INSERM, U 1059 Sainbiose, Centre CIS, F - 42023 Saint-Etienne France.
[2]INSERM U 1059 Sainbiose, Université Jean Monnet, Saint-Etienne, France.
[3]CHU Saint-Etienne, Saint-Etienne, F-42055, France.

Correspondence and requests for materials should be addressed to J.P. (email: pourchez@emse.fr)

Keywords: *ex vivo* model, e-cigarette, aerosol deposition, gamma-camera imaging

Abstract

Aim: There is a need to bridge the data gap concerning the regional deposition of electronic nicotine delivery systems (ENDS) emissions in the airways. The present work aims to experimentally and precisely asses the aerosol regional deposition of ENDS emissions using an *ex vivo* model of lungs as a complementary approach to a determinist computational model and as an alternative to animal or human *in vivo* experiments.

Methods: The refill liquid of a recent tank generation ENDS was radiolabelled with pertechnetate sodium. Particle size distributions of the emissions – in mass and in radioactivity – were determined using a cascade impaction technique. The aerosol regional deposition in the airways was both calculated with a determinist computational model and experimentally assessed by gamma-camera imaging on a controlled breathing *ex vivo* model mimicking intrapleural depression thanks to generation of negative pressures in a sealed enclosure.

Results: The aerodynamic diameter of the ENDS emissions were 1.03 ± 0.11 µm and 0.87 ± 0.03 µm (mean ± SD) in radioactivity and mass, respectively. The calculations led to a thoracic deposition of 92.89 ± 0.03% and 92.74 ± 0.19% in mass and radioactivity, respectively. The experimental data of thoracic deposition obtained by quantifying the deposited aerosol with planar scintigraphy of the *ex vivo* model were 91 ± 4%.

Conclusions: The radiolabelling of the refill liquid did not affect the particle size distribution and allowed assessment of the aerosol regional deposition by two-dimensional gamma-camera imaging. When compared, no significant difference of the thoracic deposition between calculation and experimental data could be found. Moreover, data seemed to be in good accordance with previously published data. This work supports the conclusion that this preclinical respiratory model could be used to assess regional deposition of aerosol generated by an ENDS.

Introduction

Electronic nicotine delivery systems (ENDS) – also called electronic cigarettes or e-cigarettes – are a user-driven aerosol technology, which was first patented in early 2000's by Hon Lik (Grana Rachel et al., 2014). ENDS are a rapidly emerging and diversified product class (Williams & Talbot, 2019). Basically, ENDS are battery-powered personal vaporizers. The physical principle shared by all ENDS is an electrically powered heating element which vaporises a liquid solution. Thus, an aerosol is produced and available to be inhaled. The refill liquid of an ENDS contains humectants (*i.e.* glycerol

and propylene glycol) and optional ingredients in small quantities (nicotine, water, ethanol, flavorings, etc.).

Claimed as a substitute for combustible cigarettes with a less harmful outcome, ENDS raised a controversy in the scientific and medical community. Indeed, despite containing less carcinogenic constituents than conventional cigarettes (Flora et al., 2016; Fuoco et al., 2014; Palazzolo, 2013; Sood et al., 2018), health concerns are questioned due to the lack of robust clinical evidence about long-term outcomes and especially about potential risks associated with ENDS use (Caldwell et al., 2012; Flora et al., 2016; Fuoco et al., 2014; Kosmider et al., 2020; Olmedo et al., 2018; Palazzolo, 2013; Smith et al., 2019; Visser et al., 2019). The vaping industry has seen a huge business increase during the last decade, representing billions of dollars worldwide and millions users (Palazzolo, 2013). This growing market is facing regulatory issues as regulators struggle to catch up with the fast development of new ENDS (Fuoco et al., 2014; Palazzolo, 2013; Williams & Talbot, 2019). Currently, most ENDS are regulated as general consumer products and not as medical devices. However, in some countries such as the United Kingdom, some ENDS are licensed as a medical product for smoking cessation – as a class IIa medical device – according to Directive 93/42/EC (MHRA, 2017; E-Voke 10mg and 15mg Electronic Inhaler, 2015).

Therefore, this area of research concentrated interests from the aerosol sciences community to bridge the data gap and reach a consensus concerning some scientific issues as the particle size distribution of ENDS emissions and the aerosol regional deposition (Fuoco et al., 2014; Palazzolo, 2013). Indeed, one of the main pitfalls of ENDS assessment is intrinsically related to the aerosol generated. This aerosol is composed of a dynamic mixture of gas and solvent droplets (Ingebrethsen et al., 2012; Kleinstreuer & Feng, 2013), mainly composed of a mixture of propylene glycol (PG) and vegetable glycerine (VG) acting as an airborne carrier for nicotine (Glasser et al., 2017; Thornburg, 2017). Thus, the experimental assessment of the particle size distribution of ENDS aerosol remains a challenge because of the high hygroscopicity and volatile nature of the particulate matter (Ingebrethsen et al., 2012; Manigrasso, Buonanno, Fuoco, et al., 2015; Manigrasso, Buonanno, Stabile, et al., 2015; Manigrasso et al., 2017; Mikheev et al., 2016; Oldham et al., 2018; Son et al., 2019; Sosnowski et al., 2018; Sosnowski & Kramek-Romanowska, 2016; Sundahl et al., 2017). These obstacles seriously complicate the use of sizing techniques requiring a high degree of aerosol dilution, which are expected to induce a significant particle evaporation. This corresponds to a potential bias due to the alteration of the particle size distribution compared to the one provided to the user. Additionally, the dynamic behaviour of the ENDS aerosol is expected after aerosol generation and after inhalation. Particle size distribution and particle concentration are expected to evolve due to condensational growth, particulate matter evaporation, coagulation and particle deposition. Lastly, the assessment of the particle size distribution is also particularly tricky due to the number of existing ENDS devices refill liquids, whose composition modifies of the aerodynamic features (Ooi et al., 2019; Pourchez et al., 2018; Zervas et al., 2018; Zhao et al., 2018).

Determining the aerodynamic size of ENDS emissions has a strong importance because these data are mandatory to run the existing semi-empirical and computational flow dynamic models estimating the aerosol regional deposition into the lungs (Kleinstreuer & Feng, 2013; Thornburg, 2017). Another entry needed for these models is the puffing regimen, which is also a controversial subject in research papers (Kleinstreuer & Feng, 2013; Son et al., 2019; Vansickel et al., 2018). Therefore, it remains difficult to use experimental aerodynamic data to calculate – using well-known computational model – a precise exposure dose and lung regional deposition profile to estimate with a high and robust confidence level the potential outcomes of ENDS use (Bertholon et al., 2013;

Manigrasso, Buonanno, Fuoco, et al., 2015; Palazzolo, 2013; Son et al., 2019; Sosnowski & Kramek-Romanowska, 2016; Sundahl et al., 2017; Zhang et al., 2013).

As a complementary approach to semi-empirical and/or computational flow dynamics software, the aim of this work was to experimentally and precisely assess the aerosol regional deposition of ENDS emissions. Thus, an *ex vivo* respiratory model composed of an Ear-Nose-Throat (ENT) replica of healthy adult upper airways and a porcine respiratory tract, placed in a sealed enclosure, was used (Perinel et al., 2016, 2017). Passive ventilation was performed thanks to a depression generator, producing negative pressures in the enclosure. First, we needed to radiolabel the refill liquids with a radionuclide. This radiolabelling was validated by determining the aerodynamic size distribution of radiolabelled aerosols generated by a recent tank generation ENDS. Then, we assessed the aerosol regional deposition on the *ex vivo* model by gamma-camera imaging. The reliability of the obtained data was evaluated by comparison with the literature and by running the multiple path particle dosimetry (MPPD) model.

1. Material and methods

1. Materials

As previously described (Pourchez et al., 2018), the high-power ENDS used for this study was composed of a lithium-ion battery iStick TC40W (2600 mAh, Eleaf, Shenzen, China), a GS Air 2 atomiser (Eleaf, Shenzen, China) and a GS Air pure cotton head wick (0.75 Ω, kanthal heating wire, Eleaf, Shenzen, China). All components were purchased in a local specialised store. For all experiments, the atomiser was filled with at least 2 g of refill liquid, the power of the ENDS was set at 10 W and the airflow ring was removed to prevent any "dry hit" (*i.e.* user puffing without sufficient amount of refill liquid in the wick, leading to overheat and potential damages).

The refill liquid was prepared from 100-PG base and 100-VG base (Arômes et Liquides, Andrézieux-Bouthéon, France). Both bases were purchased from a local supplier as commercial grade to be as close as possible to real use. The surfactant Tween® 80 was purchased from Sigma-Aldrich (CAS 9005-65-6, Saint-Louis, Mo., USA). About 100 MBq of sodium pertechnetate (^{99m}Tc) were taken off from a Tekcis® generator (Curium, Paris, France) located in the Nuclear Medicine department of the Saint-Etienne hospital. Absolute ethanol (EtOH) was purchased from VWR (Fontenay-sous-Bois, France).

2. Radiolabelling of ENDS refill liquid

The refill liquid was prepared from bulk components in the following mass proportions: 74% PG, 14% VG, 5% ^{99m}Tc, 4% Tween® 80 and 3% EtOH.

Bulk components were weighed with precision scales (Adventurer Pro, OHAUS, Parsippany, USA) and homogenised thanks to a stirring plate and magnetic bar in a 20 mL scintillation vial. First, PG, VG, Tween® 80 and EtOH were homogenised and kept under constant stirring. Then, ^{99m}Tc was added in the radiopharmacy laboratory in the Nuclear Medicine department of the Saint-Etienne University Hospital. The mixture was stirred for at least 10 minutes. Just before experiments, at least 2 g of radiolabelled refill liquid were placed in the reservoir of the atomiser.

3. Puffing regimen

An in-house interface was previously developed to reproducibly introduce a puff that was well-controlled for duration and volume (Bertrand et al., 2018; Pourchez et al., 2017; Prévôt et al., 2017). The puffing regimen – called AFNOR regimen – was as follows: 55-mL puff volume, 4 s puff duration, 30-s inter-puff interval, 25 puffs per series, 300-s inter-series interval as described in the AFNOR standard XP D90-300-1.

4. Particle size determination

The methodology was previously described and validated (Bertrand et al., 2018; Pourchez et al., 2017, 2018; Prévôt et al., 2017). The assessment of the aerodynamic size distribution was performed in triplicate using a DLPI cascade impactor (Dekati Low Pressure Impactor, Dekati Ltd., Kangasala, Finland) operating at an airflow of 10 L/min. The DLPI allowed aerosolised particles to be sorted into 12 aerodynamic size groups (from 30 nm to 10 µm).

The aerosol generated by the e-cigarette was sampled and transferred to the DLPI through a metal United States Pharmacopeia (USP) like artificial throat (height 112 mm; width 42 mm; internal diameter 19 mm) with a previously described in-house interface (Pourchez et al., 2017, 2018). The deposited fraction on each DLPI stage was collected on an impermeable plastic cover. This cover was then removed and the amount of ^{99m}Tc quantified using Packard Cobra II auto-gamma counting system (Perkin-Elmer, Waltham, MA, USA). Finally, the activity median aerodynamic diameter (AMAD) and the geometric standard deviation (GSD) of the aerosolised particles were calculated, according to European Pharmacopeia 2.9.18. GSD is determined by the ratio of the provisional size at the 84th percentile of the distribution to the provisional size at the 16th percentile. Between each puff, the DPLI was turned off to reduce potential evaporation of the collected particles. The mass median aerodynamic diameter (MMAD) and the subsequent GSD were determined by gravimetric measurement of each stage. For these experiments, 25 puffs with AFNOR regimen were performed.

5. Calculation of aerosol deposition using computational model

Estimation of the deposition of ENDS emissions in the human airways was carried out using the Multiple Path Particle Dosimetry software (MPPD v3.04, ARA, Arlington, VA, USA). Introduced parameters were obtained from the work of Son *et al.* (Son et al., 2019). Some parameters such as puff volume, aerosol density, AMAD/MMAD and GSD were obtained from data generated in the present study.

We used the Yeh & Schum symmetric airway morphometry with a functional residual capacity of 3300 mL and upper respiratory tract volume of 50 mL. The density of the aerosol was set at 1.07086 g/mL, while the MMAD and GSD was obtained from experimental data. Shape factor was set at 1. We used constant exposure scenario, allowing the supine position inhalation. Aerosol concentration was set at 36181 according to experimental data of cascade impaction. Breathing frequency was set at 15 cycle/min with 500 mL of tidal volume and an inspiratory fraction of 0.33 with oral breathing, according to the experimental settings.

6. Experimental assessment of regional aerosol deposition using an *ex vivo* respiratory model

To assess the regional deposition of the aerosol generated with an ENDS, the refill liquid was labelled with 400 MBq of sodium pertechnetate. To assure enough deposition and, thus, a quantitative assessment of the deposited dose, 100 puffs were sampled – according to the puffing regimen described above – to be inhaled by the *ex vivo* respiratory model. To ensure inhalation of ENDS emissions, each puff was manually synchronized with a deep inspiration over 4s. The human-like model is composed of a 3D-printed Ear-Nose-Throat (ENT) replica (female subject, 27 years old) connected to a sealed enclosure. The ENT presents a naso-buccal breathing but for the purposes of this study, nasal orifices were occluded to ensure strict oral breathing. Within this enclosure, an *ex vivo* porcine respiratory tract is passively ventilated thanks to a SuperDimension® depression generator (Covidien, Dusseldorf, Germany), which applied negative pressure in the enclosure (mean depression -9 kPa). Respiratory parameters were previously described (Crémillieux et al., 2020; Montigaud, Perinel-Ragey, et al., 2019): 15 cycles per min, with 1.33 s inspiratory time and 2.66 s

expiratory time leading to inspiratory/expiratory ratio of 1:2 inducing tidal volume about 500 mL and dynamic compliance about 90 cmH_2O/mL. All experiments with the *ex vivo* model were performed at isothermal laboratory temperature.

Detailed collection, preparation and storage protocols were extensively described in previously work of our group (Montigaud, Georges, et al., 2019, 2019; Perinel et al., 2016, 2017). Briefly, all respiratory tracts, collected from a local slaughterhouse, passed all quality controls according to French regulation. At slaughtering time, swine were 6 months old, with 44% of female and 56% of male from three different species: large white, pietrain and landrace (with mainly large white). After removal of viscera, carcasses weighted 90 to 93kg. Visual controls of wounds and sutures were achieved, and a bronchoscopy was performed to ensure the absence of significant obstruction of proximal bronchi.

The gamma-camera imaging was performed as previously described (Montigaud, Perinel-Ragey, et al., 2019; Perinel et al., 2016). Briefly, two-dimension scintigraphies were conducted on 3 respiratory tracts with a variable angle dual detector Single Photon Emission Computed Tomography/Computed Tomography (SPECT-CT, SYMBIA T2; Siemens, Knoxville, TN, USA). After inhalation of the aerosol, each component of the system was imaged with 3-min anterior/posterior exposition: e-cigarette, expiratory filter, ENT replica and respiratory tract. The count of each part was determined with corrections for background radiation, radioactivity decay and tissue attenuation (correction factor calculated for each component). Results were expressed in terms of the total deposited dose of radioactivity in the respiratory tract and the ENT or as proportion of inhaled dose, which corresponds to the sum of deposited aerosol in the ENT, the respiratory tract and the exhaled filter. The central-to-peripheral ratio (C/P ratio) and its inverse, the penetration index (PI), were calculated as previously described (Montigaud, Georges, et al., 2019; Newman et al., 2012).

7. Statistical analysis

Statistical analyses were performed with GraphPad Prism 8 software. For the aerodynamic size distribution, a non-parametric Kolmogorov-Smirnov test was used. For the comparison of the regional deposition experimentally obtained and estimated with the MPPD software, a two-way ANOVA was used with a Tukey's multiple comparison *post-hoc* test.

Results

1. Particle size distribution

The aerodynamic size distribution was used to determine the MMAD and the AMAD of the ENDS emissions. Figure 1 presents the distribution of the radiolabelled droplets thanks to a DLPI cascade impactor. As easily seen, there is a strong recovery of the 2 curves. Table 1 presents the obtained AMAD and MMAD, with respective GSD. No significant difference between the two curves was observed (p=0.5696).

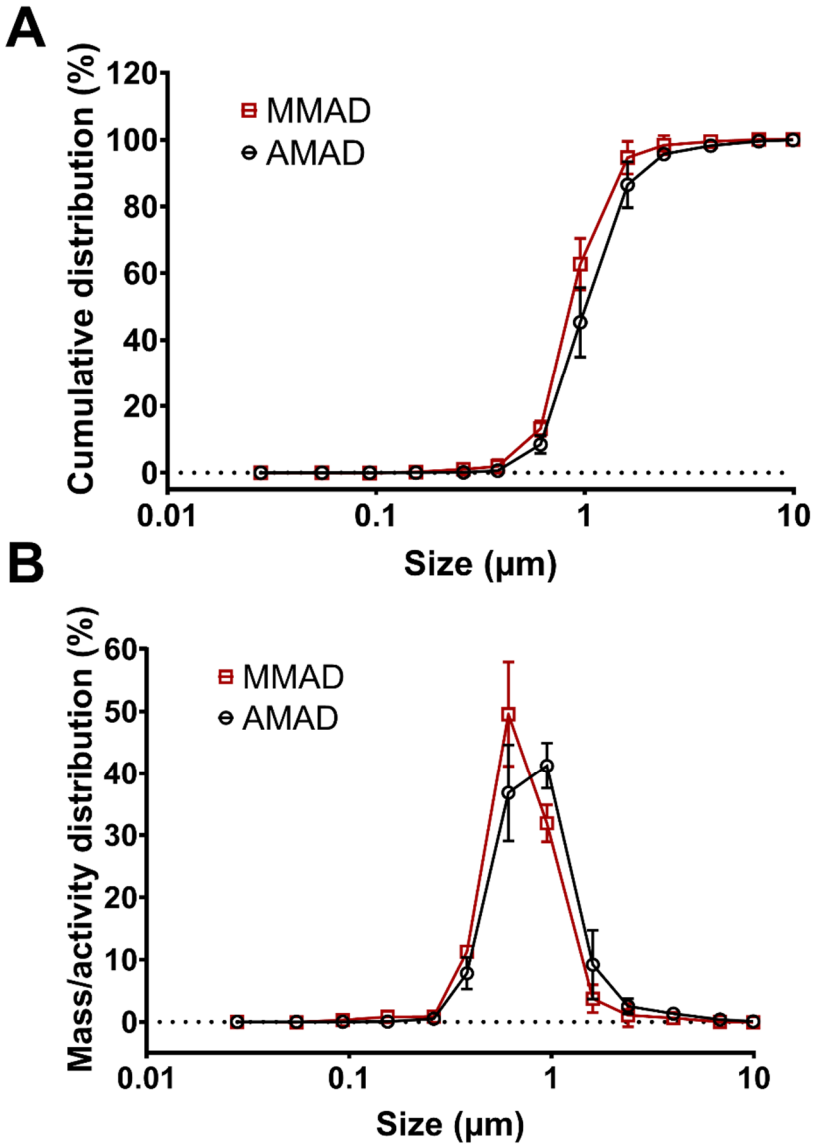

Figure 1 - A: cumulative frequency of mass or radioactivity distribution (n=3). B: frequency of mass or radioactivity distribution. Data are presented as mean ± standard deviation (SD) of the total deposited fraction in the apparatus (n=3). MMAD: Mass Median Aerodynamic Diameter. AMAD: Activity Median Aerodynamic Diameter.

Table 1 – Aerodynamic size assessment of aerosols emitted with an ENDS. Data are presented as mean ± standard deviation (SD) of a triplicate. MMAD: Mass Median Aerodynamic Diameter. AMAD: Activity Median Aerodynamic Diameter.

	MMAD	AMAD
Size (µm)	0.87 ± 0.03	1.03 ± 0.11
GSD	1.47 ± 0.05	1.53 ± 0.05

2. Aerosol regional deposition using an *ex vivo* respiratory model

The regional aerosol deposition was assessed with our innovative *ex vivo* respiratory model. One hundred puffs were used with the AFNOR regimen. Figure 2 presents the images obtained with planar scintigraphies. A homogenous deposition could be observed in the respiratory tract, as also shown by the Table S1. It is important to note that the hot-spots in Figure 2 correspond to cuts in the respiratory tract due to the sacrifice of the animal at the slaughterhouse. Therefore, it collected more aerosol due to the decreased resistance in these areas. This point corresponds to an intrinsic artefact

of the respiratory model that was extensively acknowledged in previously published works but does not significantly modify the overall aerosol regional deposition within the model (Montigaud, Georges, et al., 2019; Montigaud, Périnel-Ragey, et al., 2019; Perinel et al., 2016, 2017).

When expressed as a percentage of the total aerosol deposited dose in the respiratory tract, the fraction in the lungs represents about 90% of the deposited dose, while the ENT collected 10% of the deposited dose (Table 2). The C/P ratio of the *ex vivo* model was 0.75 of the deposited dose in the respiratory tract.

When expressed as a proportion of total inhaled dose (Table 3), the deposition pattern remained similar: most of the aerosol found in the lungs (84% ± 8), while the rest of the aerosol is partitioned between exhaled fraction (7% ± 6) and deposited fraction in the interface and upper airways (8% ± 3).

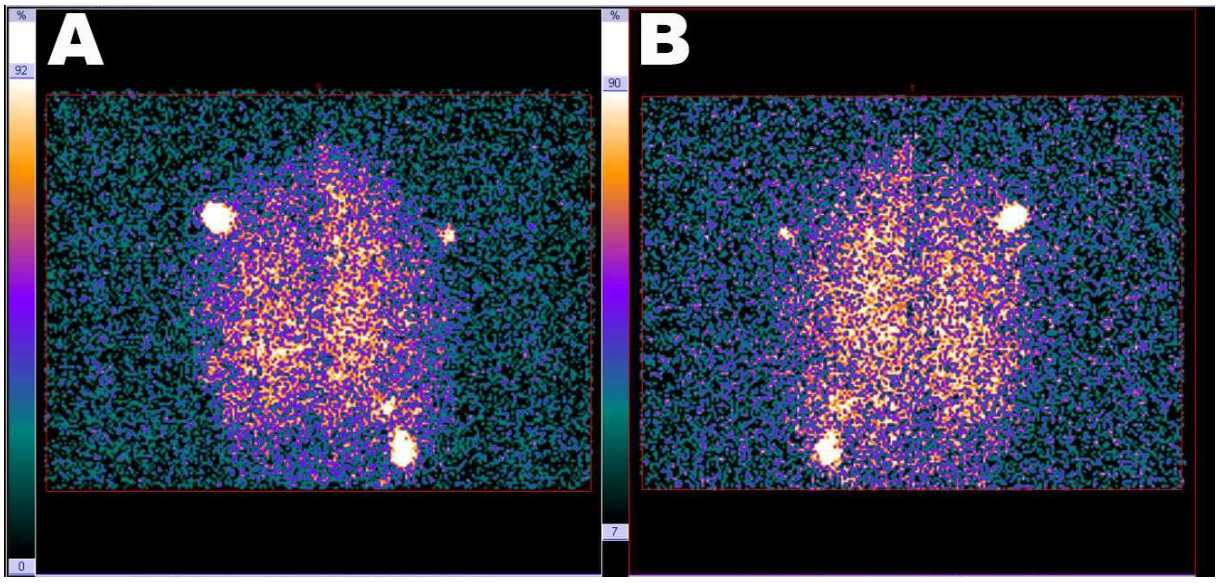

Figure 2 – Planar scintigraphies of a respiratory tract after inhalation of 100 radiolabelled puffs ENDS emissions. A: anterior acquisition. B: posterior acquisition. Hot spots correspond to cuts in the respiratory tract and, therefore, collected more aerosol due to the decreased resistance in these areas.

3. Estimation of aerosol deposition using computational model

The estimation of the deposited doses in the respiratory tract was performed with the MPPD implemented with the AFNOR puffing regimen and the AMAD or the MMAD of the emitted aerosol. The other parameters were taken from a published paper (Son et al., 2019). Figure 3 presents the different deposited fractions of the aerosol along the airways up to the pulmonary region. As presented, over 70% of the aerosol is exhaled, while the remaining aerosols is partitioned between the head, the tracheobronchial tree and the pulmonary region. Figure 3 presents the comparison of experimental and estimated data. We only considered the deposited doses in the *ex vivo* model in this comparison. No significant difference could be found between the estimated deposition obtained with AMAD and MMAD as entries, as well as for our experimental data ($p>0.9999$; Table 2 and Figure 3). Penetration of the aerosol was assessed by the determination of the C/P ratio, which were 0.7495 ± 0.0203 and 0.6942 ± 0.0365 for the estimation based on the MMAD and the AMAD, respectively, as expressed as a proportion of the total deposited dose in the respiratory tract (Table 3).

When the deposition pattern is expressed as proportion of the inhaled dose, as presented in Table 3, we could see that the exhaled fraction is over 80% (85.24% ± 0.72 and 82.86% ± 1.79 for the

estimation based on the MMAD and the AMAD, respectively). Lung deposition is about 15% (13.71% ± 0.67 and 15.90% ± 1.64 for the estimation based on the MMAD and the AMAD, respectively). The upper airway deposition is about 1% (1.05% ± 0.06 and 1.25% ± 0.15 for the estimation based on the MMAD and the AMAD, respectively).

Table 2 - Regional aerosol deposition expressed as mean ± standard deviation (SD) of the percentage of total deposited aerosol for computational model with AMAD and MMAD as inputs or for experimental results presented in this study. Extra-thoracic: ENT replica + mouth interface equivalent to head deposition in the determinist computational model. Thoracic: respiratory tract equivalent to the sum of tracheobronchial and peripheral deposition in the determinist computational model.

	MPPD estimation from MMAD	**MPPD estimation from AMAD**	**Experimental results (n=3)**
Extra-thoracic deposition	7.11% ± 0.03	7.26% ± 0.19	9% ± 4
Thoracic deposition	92.89% ± 0.03	92.74% ± 0.19	91% ± 4

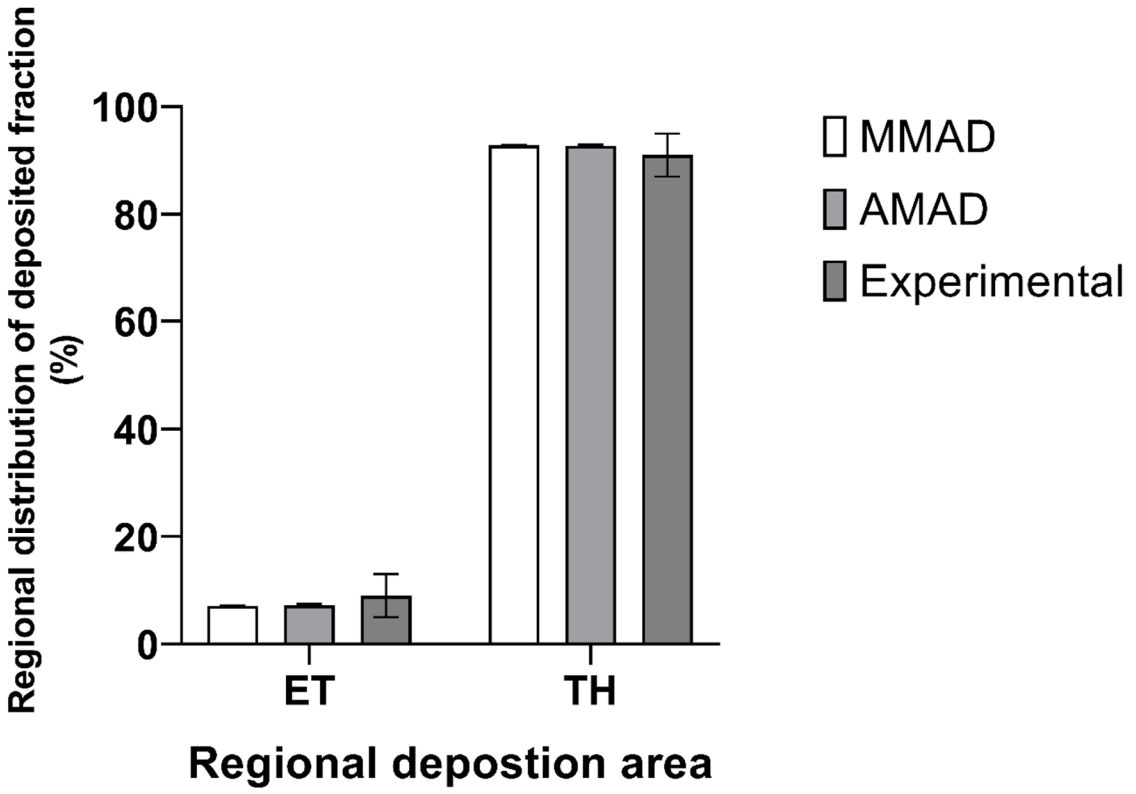

Figure 3 - MPPD estimation with MMAD or AMAD as input and experimental results of the deposition of emission of the chosen ENDS. Data are presented as mean ± standard deviation (SD) of the percentage of total deposited aerosol. ET: extra-thoracic region (head and mouthpiece). TH: thoracic region (tracheobronchial tree + peripheral lungs). MMAD: Mass Median Aerodynamic Diameter. AMAD: Activity Median Aerodynamic Diameter.

Table 3 – Homogeneity and penetration of the aerosol deposition expressed as mean ± standard deviation (SD) of the percentage of total inhaled aerosol for computational model with AMAD and MMAD as inputs or for experimental results presented in this study. Interface: in-house mouth interface. ENT: human head replica. Lungs: tracheobronchial + pulmonary deposition. Exhaled: fraction collected on the respiratory filter or as the complementary to one of the deposited fractions. C/P: central-to-peripheral ratio. PI: penetration index.

	Deposited fraction of the aerosol expressed as proportion of the inhaled dose (%)			**Regionalisation of the deposition/penetration of the aerosol in the respiratory tract**		
	Interface + ENT	**Exhaled**	**Lungs**	**C/P ratio**	**PI**	**Left/right ratio**
Experimental data	8 ± 3	7 ± 6	84 ± 8	0.75 (n=1)	1.33 (n=1)	1.00 (n=1)
Estimation from MMAD	1.05 ± 0.06	85.24 ± 0.72	13.71 ± 0.67	0.7495 ± 0.0203 (n=3)	1.3348 ± 0.0366 (n=3)	N/A
Estimation from AMAD	1.25 ± 0.15	82.86 ± 1.79	15.90 ± 1.64	0.6942 ± 0.0365 (n=3)	1.4432 ± 0.0759 (n=3)	N/A

Discussion

1. Particle size distribution

To our knowledge, only one study was conducted on radiolabelled aerosol emitted with an ENDS (Holbrook et al., 2018). In this work, the aerosol is radiolabelled by a complex process with technetium solid particles incorporated in the ENDS emissions. Despite being an ingenious way to radiolabel the aerosol, this method seems not to be suitable for extensive studies. The method presented in this work seems to be easier as it only needs to introduce a radionuclide – pertechnetate ions ($^{99m}TcO_4^-$) – in the refill liquid. With a MMAD of 0.87 ± 0.03 µm and an AMAD of 1.03 ± 0.11 µm, we considered that the two aerodynamic sizes are equivalent. This assumption is supported by the absence of significant difference of the distributions obtained with a cascade impactor (p=0.5696). Therefore, one could assume that the radiolabelling was efficient and does not modify the airborne properties of the ENDS emissions. These aerodynamic sizes are coherent with data found in literature, when cascade impactors are used (Holbrook et al., 2018; Mulder et al., 2019; Oldham et al., 2018; Pourchez et al., 2018; Sundahl et al., 2017; Zhao et al., 2018).

While the presented data are coherent with literature for cascade impactor measurement, they fall in the wide controversy concerning the aerodynamic size determination and concerning the lack standardized methods for this assessment (Ingebrethsen et al., 2012). Indeed, when particle count and light scattering methods are used, the aerodynamic size distribution appeared to be bimodal with a mode composed of small nanoparticles between 10 to 100 nm and another of submicronic particles with a size 2-fold lower than the MMAD and AMAD found in this study (Nordlund et al., 2017; Pratte et al., 2016; Son et al., 2019). However, due to the high concentration of droplets in the aerosol, these methods required to dilute the aerosol and, thus, it is acknowledged that this particular point is a bias leading to a underestimation of the size of the droplets (Bertholon et al., 2013; Ingebrethsen et al., 2012). This is due to a dynamic evaporation process induced by the volatile

and semi-volatile components of the refill liquids (Caldwell et al., 2012; Glasser et al., 2017; Sosnowski & Odziomek, 2018).

Lastly, it is important to be noted that there is an important variability of ENDS technical features and refill liquids. The main point of variation of the ENDS is due to the power generated by the battery and the coil, while the composition of the refill liquids would influence the dynamic behaviour of the e-cigarette aerosols (Floyd et al., 2018; Mulder et al., 2019; Olmedo et al., 2018; Ooi et al., 2019).

2. Aerosol regional deposition of ENDS emissions: modelling *vs.* experimental

In this study, about 90% of the deposited dose was found to the thoracic regions (Table 2). Moreover, our estimation based on the experimentally determined AMAD and MMAD led to similar modelled results, which were not significantly different from the experimental data generated with the *ex vivo* model. This findings seems to be coherent with some modelled data of the literature, where e-cigarette and conventional cigarette aerosol deposition are estimated to deposit up to 90% in the thoracic region (Son et al., 2019; Sundahl et al., 2017). However, these findings seem to be similar when only expressed as proportion of the total deposited dose. Moreover, comparison should be done cautiously, as the breathing pattern and the airway morphometry used to estimate the values could be different, which would generate comparison biases.

Indeed, when the results are expressed as a proportion of the total inhaled dose (*i.e.* the sum of the radioactivity found in the respiratory tract, the upper airways and in the exhaled filters). In this case the experimental data did not match with estimated values obtained with the MPPD or the literature, where 70 to 90 % of the aerosol is found to be exhaled (Son et al., 2019; Sundahl et al., 2017). In the present study, only 7% is found in the exhaled filter for experimental data, while over 80% of the aerosol is exhaled according to the MPPD. (Table 3). These discrepancies between the experimental and estimated values seem to be problematic because it is hard to determine, which model is similar to reality. However, while most of the estimation are agreeing on a high exhaled fraction, the study from St. Helen *et al.* showed interesting "deposition data" on healthy volunteers. In their study, the retained dose of PG, VG and nicotine as well as the exhaled dose of the same components were assessed. They found that the retained dose, equivalent to the deposited dose, of the aerosol was about 93.8 ± 14.4% for the nicotine, 84.4 ± 26.4% for the VG and 91.7 ± 15.9% for the PG (St. Helen et al., 2016). Interestingly, these real-life data are in opposition with estimated data while they appeared to be similar to the present experimental values. One could think that determinist computational model are not accurate enough, due to some biases in the model itself.

However, further studies are needed to validate both the estimation by a determinist computational model, such as the MPPD, and expedata obtained, such as St. Helen *et al.* or the present study, and to reconcile computational and experimental data. Particularly, hygroscopic growth and condensation phenomena, as well as vapour-gas equilibrium and deposition mechanisms involved (James F. Pankow, 2001; James F. Pankow et al., 2003), should be better understood to predict the outcomes of the exposure to an aerosol emitted by ENDS.

It is interesting to note that, even if the regionalisation of the deposition is not accurate between experimental data, when expressed as proportion of the inhaled dose, the penetration of the aerosol tend to be similar. Indeed, for the *ex vivo* model the C/P ratio was 0.75, while it was between 0.70-0.75 for the estimation with the MPPD.

Therefore, despite being questionable to assess the exhaled dose, the *ex vivo* respiratory model appeared to be a potential tool of interest to assess regional deposition and the penetration of aerosol emitted with an ENDS. Moreover, this model already proved to be an interesting surrogate

preclinical model to animal experiments by respecting the 3Rs concept and therefore being ethically less restricted (National Center for Replacement, Reduction and Refinement of Animal Research, 2018; Perinel et al., 2016, 2017). Despite the improvements that could be added to the model, such as an automated aerosol sample or the vertical position of the respiratory tract. Indeed, the supine position of the *ex vivo* model is a known limit of the model that could lead to overestimate the deposited fraction in the respiratory tract. However, we hope that this new tool would be a new step to assess the deposition of e-cigarette aerosols and to help to produce strong and reliable scientific evidence concerning the outcomes of ENDS.

Conclusion

Through this study, we aimed to assess the regional deposition of an aerosol generated with a high-power ENDS. First, we had to radiolabel the refill liquid with pertechnetate sodium solution, which was achieved thanks to the use of a commonly used surfactant. To validate this point, we studied the recovery of the MMAD and the AMAD using a DLPI cascade impactor. No significant difference could be found between these two aerodynamic distributions. Then, we assessed the regional aerosol deposition with a preclinical *ex vivo* respiratory model. Pulmonary deposition (91 ± 4%) was coherent with data described in literature using semi-empirical/computational fluid dynamics software (Sundahl et al., 2017; Zhang et al., 2013). Lastly, we compared the estimated deposition available in published data with our experimental data and with estimated values obtained by running the MPPD software, which appeared to be in the same range of commonly acknowledged values (Manigrasso, Buonanno, Fuoco, et al., 2015; Manigrasso, Buonanno, Stabile, et al., 2015; Son et al., 2019; Sosnowski & Kramek-Romanowska, 2016; Sundahl et al., 2017; Zhang et al., 2013). Therefore, we supported that this preclinical model could be used to assess regional deposition of aerosol generated with an ENDS. We hope that this work will allow the generation of strong evidences to fill the data gap concerning the outcomes of ENDS.

Acknowledgement

Authors would like to kindly thank the slaughterhouse DespiViandes (La Talaudière France) for supplying the porcine respiratory tracts.

Funding source

This work was funded by a grant from the French National Agency for Research [ANR-17-CE19-0002-01].

Declaration of interest

JP works as expert on electronic cigarette risk assessment for the French Agency for Food, Environmental and Occupational Health & Safety (ANSES).

Other authors report no conflict of interest concerning the present study.

References

Bertholon, J.-F., Becquemin, M. H., Roy, M., Roy, F., Ledur, D., Annesi Maesano, I., & Dautzenberg, B. (2013). Comparaison de l'aérosol de la cigarette électronique à celui des cigarettes ordinaires et de la chicha. *Revue Des Maladies Respiratoires*, *30*(9), 752–757. https://doi.org/10.1016/j.rmr.2013.03.003

Bertrand, P., Bonnarme, V., Piccirilli, A., Ayrault, P., Lemée, L., Frapper, G., & Pourchez, J. (2018). Physical and chemical assessment of 1,3 Propanediol as a potential substitute of propylene glycol in refill liquid for electronic cigarettes. *Scientific Reports*, *8*(1), 1–10. https://doi.org/10.1038/s41598-018-29066-6

Caldwell, B., Sumner, W., & Crane, J. (2012). A Systematic Review of Nicotine by Inhalation: Is There a Role for the Inhaled Route? *Nicotine & Tobacco Research*, *14*(10), 1127–1139. https://doi.org/10.1093/ntr/nts009

Crémillieux, Y., Montigaud, Y., Bal, C., Pinaud, N., Pham, V., Perinel, S., Natuzzi, M., Lux, F., Tillement, O., Ichinose, N., Zhang, B., & Pourchez, J. (2020). Three-dimensional quantitative MRI of aerosolized gadolinium-based nanoparticles and contrast agents in isolated ventilated porcine lungs. *Magnetic Resonance in Medicine*, *83*(5), 1774–1782. https://doi.org/10.1002/mrm.28041

Flora, J. W., Meruva, N., Huang, C. B., Wilkinson, C. T., Ballentine, R., Smith, D. C., Werley, M. S., & McKinney, W. J. (2016). Characterization of potential impurities and degradation products in electronic cigarette formulations and aerosols. *Regulatory Toxicology and Pharmacology*, *74*, 1–11. https://doi.org/10.1016/j.yrtph.2015.11.009

Floyd, E. L., Queimado, L., Wang, J., Regens, J. L., & Johnson, D. L. (2018). Electronic cigarette power affects count concentration and particle size distribution of vaping aerosol. *PLOS ONE*, *13*(12), e0210147. https://doi.org/10.1371/journal.pone.0210147

Fuoco, F. C., Buonanno, G., Stabile, L., & Vigo, P. (2014). Influential parameters on particle concentration and size distribution in the mainstream of e-cigarettes. *Environmental Pollution*, *184*, 523–529. https://doi.org/10.1016/j.envpol.2013.10.010

Glasser, A. M., Collins, L., Pearson, J. L., Abudayyeh, H., Niaura, R. S., Abrams, D. B., & Villanti, A. C. (2017). Overview of Electronic Nicotine Delivery Systems: A Systematic Review. *American Journal of Preventive Medicine*, *52*(2), e33–e66. https://doi.org/10.1016/j.amepre.2016.10.036

Grana Rachel, Benowitz Neal, & Glantz Stanton A. (2014). E-Cigarettes. *Circulation*, *129*(19), 1972–1986. https://doi.org/10.1161/CIRCULATIONAHA.114.007667

Holbrook, L. T., Zeman, K. L., Burke, A., Jaspers, I., & Bennett, W. D. (2018). Radiolabeling an Electronic Cigarette Aerosol Using Technetium Carbon Ultrafine Particles. *Journal of Aerosol Medicine and Pulmonary Drug Delivery*, *32*(1), 47–53. https://doi.org/10.1089/jamp.2017.1442

Ingebrethsen, B. J., Cole, S. K., & Alderman, S. L. (2012). Electronic cigarette aerosol particle size distribution measurements. *Inhalation Toxicology*, *24*(14), 976–984. https://doi.org/10.3109/08958378.2012.744781

Kleinstreuer, C., & Feng, Y. (2013). Lung Deposition Analyses of Inhaled Toxic Aerosols in Conventional and Less Harmful Cigarette Smoke: A Review. *International Journal of Environmental Research and Public Health*, *10*(9), 4454–4485. https://doi.org/10.3390/ijerph10094454

Kosmider, L., Cox, S., Zaciera, M., Kurek, J., Goniewicz, M. L., McRobbie, H., Kimber, C., & Dawkins, L. (2020). Daily exposure to formaldehyde and acetaldehyde and potential health risk associated with use of high and low nicotine e-liquid concentrations. *Scientific Reports*, *10*(1), 1–10. https://doi.org/10.1038/s41598-020-63292-1

Manigrasso, M., Buonanno, G., Fuoco, F. C., Stabile, L., & Avino, P. (2015). Aerosol deposition doses in the human respiratory tree of electronic cigarette smokers. *Environmental Pollution*, *196*, 257–267. https://doi.org/10.1016/j.envpol.2014.10.013

Manigrasso, M., Buonanno, G., Fuoco, F. C., Stabile, L., & Avino, P. (2017). Electronic cigarettes: age-specific generation-resolved pulmonary doses. *Environmental Science and Pollution Research*, *24*(14), 13068–13079. https://doi.org/10.1007/s11356-017-8914-8

Manigrasso, M., Buonanno, G., Stabile, L., Morawska, L., & Avino, P. (2015). Particle doses in the pulmonary lobes of electronic and conventional cigarette users. *Environmental Pollution*, *202*, 24–31. https://doi.org/10.1016/j.envpol.2015.03.008

e-Voke 10mg and 15mg Electronic Inhaler, Pub. L. No. PL 42601/0003-4, PL 42601/0003-4 PL 42601/0003-4 (2015). https://mhraproductsprod.blob.core.windows.net/docs-20200420/56f25daab2a2968139bc37075e194d1a5f12b33f

MHRA. (2017, December 14). *E-cigarettes: regulations for consumer products*. GOV.UK. https://www.gov.uk/guidance/e-cigarettes-regulations-for-consumer-products

Mikheev, V. B., Brinkman, M. C., Granville, C. A., Gordon, S. M., & Clark, P. I. (2016). Real-Time Measurement of Electronic Cigarette Aerosol Size Distribution and Metals Content Analysis. *Nicotine & Tobacco Research*, *18*(9), 1895–1902. https://doi.org/10.1093/ntr/ntw128

Montigaud, Y., Georges, Q., Pourchez, J., Leclerc, L., Goy, C., Clotagatide, A., Prevot, N., & Perinel-Ragey, S. (2019). Aerosol delivery during invasive mechanical ventilation: development of a preclinical ex vivo respiratory model for aerosol regional deposition. *Scientific Reports*, *9*(1), 1–9. https://doi.org/10.1038/s41598-019-54480-9

Montigaud, Y., Perinel-Ragey, S., Plantier, L., Leclerc, L., Goy, C., Clotagatide, A., Prévôt, N., & Pourchez, J. (2019). Development of an ex vivo preclinical respiratory model of idiopathic pulmonary fibrosis for aerosol regional studies. *Scientific Reports*, *9*(1), 1–11. https://doi.org/10.1038/s41598-019-54479-2

Mulder, H. A., Patterson, J. L., Halquist, M. S., Kosmider, L., Turner, J. B. M., Poklis, J. L., Poklis, A., & Peace, M. R. (2019). The Effect of Electronic Cigarette User Modifications and E-liquid Adulteration on the Particle Size Profile of an Aerosolized Product. *Scientific Reports*, *9*. https://doi.org/10.1038/s41598-019-46387-2

National Center for Replacement, Reduction and Refinement of Animal Research. (2018, August 13). *The 3Rs | NC3Rs*. https://www.nc3rs.org.uk/the-3rs

Newman, S., Bennett, W. D., Biddiscombe, M., Devadason, S. G., Dolovich, M. B., Fleming, J., Haeussermann, S., Kietzig, C., Kuehl, P. J., Laube, B. L., Sommerer, K., Taylor, G., Usmani, O. S., & Zeman, K. L. (2012). Standardization of Techniques for Using Planar (2D) Imaging for

Aerosol Deposition Assessment of Orally Inhaled Products. *Journal of Aerosol Medicine and Pulmonary Drug Delivery*, *25*(S1), S-10. https://doi.org/10.1089/jamp.2012.1Su4

Nordlund, M., Belka, M., Kuczaj, A. K., Lizal, F., Jedelsky, J., Elcner, J., Jicha, M., Sauser, Y., Bouhellec, S. L., Cosandey, S., Majeed, S., Vuillaume, G., Peitsch, M. C., & Hoeng, J. (2017). Multicomponent aerosol particle deposition in a realistic cast of the human upper respiratory tract. *Inhalation Toxicology*, *29*(3), 113–125. https://doi.org/10.1080/08958378.2017.1315196

Oldham, M. J., Zhang, J., Rusyniak, M. J., Kane, D. B., & Gardner, W. P. (2018). Particle size distribution of selected electronic nicotine delivery system products. *Food and Chemical Toxicology*, *113*, 236–240. https://doi.org/10.1016/j.fct.2018.01.045

Olmedo, P., Goessler, W., Tanda, S., Grau-Perez, M., Jarmul, S., Aherrera, A., Chen, R., Hilpert, M., Cohen, J. E., Navas-Acien, A., & Rule, A. M. (2018). Metal Concentrations in e-Cigarette Liquid and Aerosol Samples: The Contribution of Metallic Coils. *Environmental Health Perspectives*, *126*(2). https://doi.org/10.1289/EHP2175

Ooi, B. G., Dutta, D., Kazipeta, K., & Chong, N. S. (2019). Influence of the E-Cigarette Emission Profile by the Ratio of Glycerol to Propylene Glycol in E-Liquid Composition. *ACS Omega*, *4*(8), 13338–13348. https://doi.org/10.1021/acsomega.9b01504

Palazzolo, D. L. (2013). Electronic Cigarettes and Vaping: A New Challenge in Clinical Medicine and Public Health. A Literature Review. *Frontiers in Public Health*, *1*. https://doi.org/10.3389/fpubh.2013.00056

Pankow, James F. (2001). A consideration of the role of gas/particle partitioning in the deposition of nicotine and other tobacco smoke compounds in the respiratory tract. *Chemical Research in Toxicology*, *14*(11), 1465–1481. https://doi.org/10.1021/tx0100901

Pankow, James F., Tavakoli, A. D., Luo, W., & Isabelle, L. M. (2003). Percent free base nicotine in the tobacco smoke particulate matter of selected commercial and reference cigarettes. *Chemical Research in Toxicology*, *16*(8), 1014–1018. https://doi.org/10.1021/tx0340596

485 Perinel, S., Leclerc, L., Prévôt, N., Deville, A., Cottier, M., Durand, M., Vergnon, J.-M., & Pourchez, J.
486 (2016). Micron-sized and submicron-sized aerosol deposition in a new ex vivo preclinical
487 model. *Respiratory Research*, *17*. https://doi.org/10.1186/s12931-016-0395-7
488 Perinel, S., Pourchez, J., Leclerc, L., Avet, J., Durand, M., Prévôt, N., Cottier, M., & Vergnon, J. M.
489 (2017). Development of an ex vivo human-porcine respiratory model for preclinical studies.
490 *Scientific Reports*, *7*. https://doi.org/10.1038/srep43121
491 Pourchez, J., de Oliveira, F., Perinel-Ragey, S., Basset, T., Vergnon, J.-M., & Prévôt, N. (2017).
492 Assessment of new-generation high-power electronic nicotine delivery system as thermal
493 aerosol generation device for inhaled bronchodilators. *International Journal of*
494 *Pharmaceutics*, *518*(1), 264–269. https://doi.org/10.1016/j.ijpharm.2017.01.009
495 Pourchez, J., Parisse, S., Sarry, G., Perinel-Ragey, S., Vergnon, J.-M., Clotagatide, A., & Prévôt, N.
496 (2018). Impact of power level and refill liquid composition on the aerosol output and particle
497 size distribution generated by a new-generation e-cigarette device. *Aerosol Science and*
498 *Technology*, *52*(4), 359–369. https://doi.org/10.1080/02786826.2017.1422857
499 Pratte, P., Cosandey, S., & Goujon-Ginglinger, C. (2016). A scattering methodology for droplet sizing
500 of e-cigarette aerosols. *Inhalation Toxicology*, *28*(12), 537–545.
501 https://doi.org/10.1080/08958378.2016.1224956
502 Prévôt, N., Oliveira, F. de, Perinel-Ragey, S., Basset, T., Vergnon, J.-M., & Pourchez, J. (2017). Nicotine
503 delivery from the refill liquid to the aerosol via high-power e-cigarette device. *Scientific*
504 *Reports*, *7*(1), 2592. https://doi.org/10.1038/s41598-017-03008-0
505 Smith, D. M., Schneller, L. M., O'Connor, R. J., & Goniewicz, M. L. (2019). Are E-Cigarette Flavors
506 Associated with Exposure to Nicotine and Toxicants? Findings from Wave 2 of the Population
507 Assessment of Tobacco and Health (PATH) Study. *International Journal of Environmental*
508 *Research and Public Health*, *16*(24), 5055. https://doi.org/10.3390/ijerph16245055
509 Son, Y., Mainelis, G., Delnevo, C., Wackowski, O. A., Schwander, S., & Meng, Q. (2019). Investigating
510 E-Cigarette Particle Emissions and Human Airway Depositions under Various E-Cigarette-Use

Conditions. *Chemical Research in Toxicology*. https://doi.org/10.1021/acs.chemrestox.9b00243

Sood, A. K., Kesic, M. J., & Hernandez, M. L. (2018). Electronic cigarettes: One size does not fit all. *Journal of Allergy and Clinical Immunology*, *141*(6), 1973–1982. https://doi.org/10.1016/j.jaci.2018.02.029

Sosnowski, T. R., Jabłczyńska, K., Odziomek, M., Schlage, W. K., & Kuczaj, A. K. (2018). Physicochemical studies of direct interactions between lung surfactant and components of electronic cigarettes liquid mixtures. *Inhalation Toxicology*, *30*(4–5), 159–168. https://doi.org/10.1080/08958378.2018.1478916

Sosnowski, T. R., & Kramek-Romanowska, K. (2016). Predicted Deposition of E-Cigarette Aerosol in the Human Lungs. *Journal of Aerosol Medicine and Pulmonary Drug Delivery*, *29*(3), 299–309. https://doi.org/10.1089/jamp.2015.1268

Sosnowski, T. R., & Odziomek, M. (2018). Particle Size Dynamics: Toward a Better Understanding of Electronic Cigarette Aerosol Interactions With the Respiratory System. *Frontiers in Physiology*, *9*. https://doi.org/10.3389/fphys.2018.00853

St. Helen, G., Havel, C., Dempsey, D., Jacob, P., & Benowitz, N. L. (2016). Nicotine delivery, retention, and pharmacokinetics from various electronic cigarettes. *Addiction (Abingdon, England)*, *111*(3), 535–544. https://doi.org/10.1111/add.13183

Sundahl, M., Berg, E., & Svensson, M. (2017). Aerodynamic particle size distribution and dynamic properties in aerosols from electronic cigarettes. *Journal of Aerosol Science*, *103*, 141–150. https://doi.org/10.1016/j.jaerosci.2016.10.009

Thornburg, J. (2017). Chapter 3 - Exposures to e-Cigarette Vapor. In K. E. Farsalinos, I. G. Gillman, S. S. Hecht, R. Polosa, & J. Thornburg (Eds.), *Analytical Assessment of E-Cigarettes* (pp. 37–58). Elsevier. https://doi.org/10.1016/B978-0-12-811241-0.00003-6

Vansickel, A. R., Edmiston, J. S., Liang, Q., Duhon, C., Connell, C., Bennett, D., & Sarkar, M. (2018). Characterization of puff topography of a prototype electronic cigarette in adult exclusive

cigarette smokers and adult exclusive electronic cigarette users. *Regulatory Toxicology and Pharmacology*, *98*, 250–256. https://doi.org/10.1016/j.yrtph.2018.07.019

Visser, W. F., Klerx, W. N., Cremers, H. W. J. M., Ramlal, R., Schwillens, P. L., & Talhout, R. (2019). The Health Risks of Electronic Cigarette Use to Bystanders. *International Journal of Environmental Research and Public Health*, *16*(9), 1525. https://doi.org/10.3390/ijerph16091525

Williams, M., & Talbot, P. (2019). Design Features in Multiple Generations of Electronic Cigarette Atomizers. *International Journal of Environmental Research and Public Health*, *16*(16), 2904. https://doi.org/10.3390/ijerph16162904

Zervas, E., Litsiou, E., Konstantopoulos, K., Poulopoulos, S., & Katsaounou, P. (2018). Physical characterization of the aerosol of an electronic cigarette: impact of refill liquids. *Inhalation Toxicology*, *30*(6), 218–223. https://doi.org/10.1080/08958378.2018.1500662

Zhang, Y., Sumner, W., & Chen, D.-R. (2013). In Vitro Particle Size Distributions in Electronic and Conventional Cigarette Aerosols Suggest Comparable Deposition Patterns. *Nicotine & Tobacco Research*, *15*(2), 501–508. https://doi.org/10.1093/ntr/nts165

Zhao, J., Nelson, J., Dada, O., Pyrgiotakis, G., Kavouras, I. G., & Demokritou, P. (2018). Assessing electronic cigarette emissions: linking physico-chemical properties to product brand, e-liquid flavoring additives, operational voltage and user puffing patterns. *Inhalation Toxicology*, *30*(2), 78–88. https://doi.org/10.1080/08958378.2018.1450462